Journal Name

ARTICLE TYPE

Cite this: DOI: 00.0000/xxxxxxxxxx

Supporting Information for *Transient osmotic flows in a microfluidic channel: measurements of solute permeability and reflection coefficients of hydrogel membranes*

Julien Renaudeau,[a] Pierre Lidon,[a] and Jean-Baptiste Salmon[a]

Received Date
Accepted Date

DOI: 00.0000/xxxxxxxxxx

1 Fabrication of the PEGDA microfluidic chip

The microfluidic chips were made of a crosslinked PEGDA-250 matrix (average M_n, Merck) sealed by a glass slide, following the protocol of Keita et al.[1] summarized below.

We first made a mold in SU8 resin on a silicon wafer by standard 2-level photolithography. The first level contained the channels of height $h = 45\,\mu$m while the second level (thickness $H \simeq 150\,\mu$m) contained the inlets and outlets of the chip (see Fig. S1a). The mold was treated with hexamethyldisilazane (HMDS, Merck) by chemical vapor deposition ($\simeq 30$ min) to ensure its hydrophobicity. We put a glass slide on top of the second level pillars. Then, we gently deposited $\simeq 0.25$ mL of a PEGDA-250/2-hydroxy-2-methylpropiophenone (2-HMP, Merck) liquid formulation (ratio 95/5% vol.), see Fig. S1a, to fill the space between the wafer and the slide by capillarity. The liquid layer was exposed to UV light ($\lambda = 385$ nm, exposure time ≤ 1 s, illumination $P \simeq 80\,\mathrm{mW\,cm^{-2}}$, MJB4 SÜSS MicroTec) which triggers the partial crosslinking of PEGDA-250 following a chain reaction initiated by 2-HMP, see Fig. S1b. The PEGDA layer was then carefully peeled off from the mold (Fig. S1c), and bonded to a glass slide previously coated with acrylate silane (Merck) by chemical vapor deposition ($\simeq 10$ h). Finally, the chip was exposed to UV light ($\simeq 3$ min) to fully crosslink PEGDA-250 and chemically bond it to the glass slide (Fig. S1d).

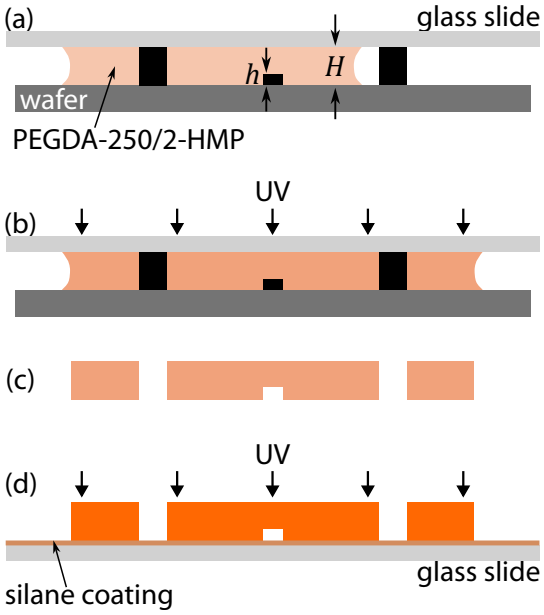

Fig. S1 Microfabrication protocol of the chips. (a) Capillary injection of the PEGDA-250/2-HMP formulation between a 2-level SU8 mold on a silicon wafer and a glass slide (height of the network of channels $h = 45\,\mu$m, height of the inlets playing the role of pillars $H \simeq 150\,\mu$m). (b) First exposure to UV light and (c) peeling of the partially crosslinked PEGDA layer from the mold. (d) Exposure to UV of the chip after its deposit on a glass slide treated using silane acrylate.

2 Hydrogel formulation

The membranes integrated inside the chip (see Sec. 3.1 in main text) are PEGDA-700 hydrogels (average M_n, Merck) crosslinked from the same formulation used by Nguyen et al.[2]. First, PEGDA-700 is mixed with 2-HMP in a volumetric ratio 90/10%. Then, this stock solution is mixed with water at a ratio 50/50% vol., and an inhibitor (hydroquinone, Merck) is added to reach a concentration of $\simeq 10\,\mathrm{g\,L^{-1}}$. As PEGDA-700 is stored at $\simeq 4\,^\circ$C to hinder its degradation, and is therefore in a solid form, it is placed at room temperature for a few hours before handling. The hydrogel formulation is stored in the dark to prevent crosslinking by ambient light.

3 Movie

The permeation of methylene blue through the hydrogel membrane is shown in Movie M1 and corresponds to the results on

[a] CNRS, Syensqo, LOF, UMR 5258, Université de Bordeaux, 178 av. Schweitzer, 33600 Pessac, France.

† Supplementary Information available. See DOI: 00.0000/00000000.

Fig. 7 in the main text.

4 Transient osmotic flows

Table S1 is a list of parameters for the experiments displayed in Fig. 9 for dextran, and Figs. 10, 11 for NaCl, sucrose, PEG-400 and PEG-1000. The molecular weight M_w and total solute concentration C_0 of the investigated solutes are listed, along with the corresponding viscosity η, diffusion coefficient in water D_s, and hydraulic permeability $\mathscr{L}_p$, of the membrane used for the experiments. For NaCl[3], sucrose[4] and PEG-400[5] the osmotic pressure is given by the van't Hoff law in this concentration range, $\Pi_0 \simeq RTC_0$, while for PEG-1000, Π_0 slightly deviates from this regime[5] and is given by the thermodynamical prediction for a dilute ideal solution, $\Pi_0 \simeq RTx_0/V_w$ with V_w the molar volume of pure water and x_0 the molar fraction of solute ($V_wC_0/x_0 \simeq 0.95$). For dextran, the values are reported for the highest concentration investigated in Fig. 9. Table S1 also reports the values of σ, kD_m and $\mathscr{L}_D$ estimated from the measurements shown in Fig. 6, 7, 10 and 11 in main text, see Sec. 4.4 and 4.5.

4.1 Verification of the constitutive equations

The model written in Sec. 2.1 holds as long as eqns (3) and (4) in the main text are satisfied, i.e., the membrane resistance to solute transport is larger than that of the channel, and the transport of solute through the membrane is only due to diffusion. Table S1 reports the values of Pe that satisfy $\mathrm{Pe} \ll 1$, except for sucrose, PEG-400 and PEG-1000. Note, however, that the advection term in eqn (2) is actually negligible when $(1-\sigma)\mathrm{Pe} \ll 1$, a condition almost valid for all the solutes studied. The values of $\mathscr{R}$ are reported in Table S1 and verify $\mathscr{R} \ll 1$ and $\mathscr{R}\mathrm{Pe} \ll 1$, except for NaCl for which we possibly expect a slight concentration gradient of solute across the width of the channel. For some cases, these assumptions are at their limit of validity ($\mathscr{R} \simeq 0.44$ for NaCl and $(1-\sigma)\mathrm{Pe} \simeq 0.42$ for PEG-400), yet data are in agreement with the exponential decay of the osmotic flux V_i predicted by the model, showing that these conditions are not as strict as proposed.

4.2 Concentration boundary layer

Following the analysis of Pedley[6], the concentration boundary layer plays a negligible role in the reservoir channel AB if eqn (9) is verified, and holds as long as the thickness of the boundary layer verifies $\delta \simeq (D_sL/\dot{\gamma})^{1/3} \ll h \sim w$, see Sec. 2.2 and Fig. 2 in the main text. Such analysis also requires that the osmotic flow does not disturb that of channel AB, and that forward osmosis dominates. The first condition corresponds to $Q_{\mathrm{osm}} \ll Q$ with $Q = \delta P/R_c$, $\delta P = P_A - P_B$ being the imposed pressure drop and R_c the hydraulic resistance of the channel, computed using its geometry[7] and the viscosity η of the flowing solution, see Table S1. The second condition corresponds to $\Delta P \sim \delta P + \delta P_{\mathrm{osm}} \ll \Pi_0$, and reduces to $\delta P \ll \Pi_0$ when the first condition is met ($\delta P_{\mathrm{osm}} \simeq R_cQ_{\mathrm{osm}}$ leading to $\delta P_{\mathrm{osm}} \ll \delta P$). As shown in Table S1, these conditions are fully satisfied in the experiments discussed in the present work.

To estimate β and δ for the experiments reported in Fig. 9, 10 and 11, we evaluated the shear rate $\dot{\gamma}$ at the membrane by:

$$\dot{\gamma} = \frac{1}{h}\int_0^h \frac{\partial V}{\partial y}(y=0,z)\mathrm{d}z. \tag{S1}$$

with the Poiseuille velocity profile $V(y,z)$ for an imposed pressure drop δP in a channel with a rectangular cross-section[7]. The values of δ are reported in Table S1 and verify $\delta \ll h$ which ensures validity of Pedley's analysis. We estimated β using the experimental value of J_v (at $t=0$ for the experiments of Figs. 10 and 11). In all cases, $\beta \ll 1$, demonstrating that the concentration boundary layer is negligible. Because of the weak dependence of β with $\dot{\gamma}$, $\beta \sim \dot{\gamma}^{-1/3}$, taking another definition of the shear rate at the membrane has little impact on the conclusion.

Table S1 List of parameters for the different osmotic agents studied. * for NaCl, $C_0 = 2C_{\mathrm{NaCl}}$, see Sec. 4.5 in main text.

	NaCl	Sucrose	PEG-400	PEG-1000	Dextran
M_w (g mol^{-1})	58	342	400	10^3	10^4
C_0 (mmol L^{-1})	$10^{3\star}$	148	253	71	47
η (mPa s)	1	1.26 [8]	1.36 [9]	5.2 [10]	12.6 [11,12]
$D_s \times 10^{10}$ (m^2 s^{-1})	18.5 [13]	4.9 [14]	4.8 [15]	3.2 [15]	0.8 [2]
Π_0 (bar)	24.5	3.6	6.2	1.8	7
$\mathscr{L}_p$ (nm s^{-1} bar^{-1})	83	66	94	94	73
w_m (μm)	31	32	30	30	32
$\kappa \times 10^{20}$ (m^2)	2.46	2.04	2.70	2.70	2.21
σ	0.33	0.81	0.79	0.98	1
$kD_m \times 10^{12}$ (m^2 s^{-1})	97.5	8.07	6.88	0.18	-
$\mathscr{L}_D$ (μm s^{-1})	3.15	0.25	0.23	0.006	-
Pe	0.21	0.79	2.00	27.5	-
$(1-\sigma)$Pe	0.14	0.15	0.42	0.55	-
$\mathscr{R}$	0.44	0.12	0.13	0.005	-
$\mathscr{R}$Pe	0.09	0.09	0.26	0.14	-
δP (mbar)	50	100	100	100	50
δP_{osm} (mbar)	0.05	0.02	0.05	0.08	0.52
$\dot{\gamma} \times 10^{-3}$ (s^{-1})	2.5	4	3.6	0.9	0.2
δ (μm)	22	12	12	19	18
β	0.02	0.01	0.02	0.01	0.24

References

1 C. Keita, Y. Hallez and J.-B. Salmon, *Phys. Rev. E*, 2021, **104**, L062601.

2 H. T. Nguyen, M. Massino, C. Keita and J.-B. Salmon, *Lab Chip*, 2020, **20**, 2383.

3 M. E. Guendouzi, A. Dinane and A. Mounir, *J. Chem. Thermodyn.*, 2001, **33**, 1059.

4 M. Starzak and S. D. Peacock, *Zuckerind.*, 1997, **122**, 380.

5 J. A. Cohen, R. Podgornik, P. L. Hansen and V. A. Parsegian,

J. Phys. Chem. B, 2009, **113**, 3709.

6 T. J. Pedley, *J. Fluid Mech.*, 1981, **107**, 281.

7 H. Bruus, *Theoretical Microfluidics*, Oxford Master Series in Physics, 2007.

8 V. Telis, J. Telis-Romero, H. Mazzotti and A. Gabas, *Int. J. Food Prop.*, 2007, **10**, 185.

9 F. Han, J. Zhang, G. Chen and X. Wei, *J. Chem. Eng. Data*, 2008, **53**, 2598.

10 P. Gonzalez-Tello, F. Camacho and G. Blazquez, *J. Chem. Eng. Data*, 1994, **39**, 611.

11 E. Antoniou and M. Tsianou, *J. Appl. Polym. Sci.*, 2012, **125**, 1681.

12 C. E. Ioan, T. Aberle and W. Burchard, *Macromolecules*, 2000, **33**, 5730.

13 S. Bouazizi and S. Nasr, *J. Mol. Liq.*, 2011, **162**, 78.

14 K. H. Jensen, J. Lee, T. Bohr and H. Bruus, *Lab Chip*, 2009, **9**, 2093.

15 K. Shimada, H. Kato, T. Saito, S. Matsuyama and S. Kinugasa, *J. Chem. Phys.*, 2005, **122**, 244914.